G. A. Richards

R. G. Logan

C. T. Meyer

R. J. Anderson

U. S. Department of Energy,
Morgantown Energy Technology Center,
Morgantown, WV 26505

Ash Deposition at Coal-Fired Gas Turbine Conditions: Surface and Combustion Temperature Effects

A study of ash deposition from a cleaned bituminous and conventional bituminous coal is presented. An electrically heated drop tube furnace is used to burn the coal and provide deposition conditions representative of proposed coal-fired gas turbines. Variations in the combustion temperature and deposit surface temperature demonstrate that surface cooling may significantly reduce ash deposition, or may provide little benefit, depending on the combustion conditions. Lower temperature combustion produced larger ash particles, with a greater fraction of ash adhering to the deposition test surface. Although the sticking coefficient was higher at the lower combustion temperature, the deposits were readily removed. A modest numerical simulation suggests that the smallest ash particles can experience significant boundary layer cooling and may account for the reduction in sticking observed at some conditions.

Introduction

The U.S. Department of Energy is currently sponsoring the development of coal-fired gas turbines, with supporting research being conducted at a number of government, private, and university laboratories (Kothari and Rekos, 1988). While significant progress has been made, a major issue to be resolved is how to reduce the detrimental effects of coal mineral ash on turbine hardware. Erosion from particulate ash may be a problem if ash residues exceed 5 μm in size, but it is believed that this problem can be controlled by limiting the size of included fines (France et al., 1984). Hot corrosion by alkali sulfates may be aggravated by the erosive loss of protective coatings, but oxidation problems are currently receiving less attention than the immediate barrier associated with reducing the deposition of ash on the turbine hardware. The deposition problem is particularly severe on the fixed turbine stators, where ash may adhere in a manner that could force engine shutdown.

The problem of ash deposition in proposed coal-fired turbines has some connection to the established problem of ash fouling in industrial boilers. However, a number of distinctions should be made between the two applications. First, in the gas turbine, ash particles arrive at the turbine blade with a high velocity, typically greater than 100 m/s. This is very different from the situation in a boiler, where particle arrival occurs at speeds on the order of 10 m/s. A second difference concerns the temperature history of arriving ash particles. In the turbine, a finely divided coal aerosol will be burned in a relatively short residence time, followed by a rapid quench with dilution air, and possibly further cooling in the boundary layer surrounding cooled airfoils. The boiler environment is relatively uneventful by comparison, with fewer abrupt changes in temperature and (typically) a lower temperature for the deposit-metal interface. The difference in temperature history means that ash morphology and composition may differ between the boiler and the turbine. Thus, earlier experience with methods to reduce boiler deposition may not meet the more stringent demands of turbine applications. The ash deposition in a gas turbine is characterized by the following mechanisms. Particles arrive at the surface with high velocity gas flow (or by particle diffusion on the suction side of the blade). Referring to Fig. 1, three mechanisms are involved in the deposition process:

- **Particle/Surface Molten Phase Adhesion.** Particles will stick to the surface if the adhesive force is sufficiently strong to overcome the energy remaining from impact, which would otherwise allow the particle to rebound.
- **Deposit Erosion.** Particles may have sufficient energy to rebound and, in addition, erode part of the existing deposit.
- **Deposit Spalling.** Particles may adhere to the deposit surface, but the deposit strength is so low that part of the deposit may occasionally spall off the surface because of aerodynamic forces, vibration, or abrasive injection cleaning (nutshelling).

Selective control of these three mechanisms may reduce ash deposition. For example, the ratio of adhering mass (particles that fail to rebound) to the total mass of particles that impact the surface, is called the sticking coefficient and has been the subject of many studies (Ross et al., 1988; Rosner and Na-

Contributed by the International Gas Turbine Institute for publication in the JOURNAL OF ENGINEERING FOR GAS TURBINES AND POWER. Manuscript received at ASME Headquarters January 1991.

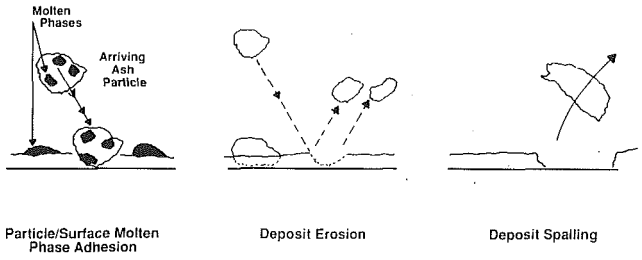

Fig. 1 Mechanisms in ash deposition

garajan, 1987; Benson et al., 1985; Ahluwalia et al., 1989). Reductions in the sticking coefficient will clearly provide an advantage to turbine operation, since a smaller proportion of the impacting ash particles will actually deposit on the hardware.

Aside from reducing the sticking coefficient, deposition control may also be accomplished by promoting deposit spalling of weakly bound ash layers. Boiler experience has included some attempts to reduce the deposit strength by intermittent injections of various additives (Raask, 1985). Spiro et al. (1989) have recently proposed that kaolin clay will act to reduce deposit strength through chemical reactions that are suspected to devitrify the deposit melt. An accompanying increase in viscosity and reduction in molar volume were thought to cause spontaneous deposit spalling. Initial tests with kaolin in a simulated turbine environment provided remarkable evidence that kaolin is effective at reducing the deposition problem (Spiro et al., 1989).

To expedite the ongoing development of coal-burning gas turbines, continued work is needed to quantify the nature of the ash deposition and potential deposition reduction schemes. While useful data have been obtained from turbine simulators (Ahluwalia et al., 1989; Spiro et al., 1989), the cost and complexity of such experiments hinder the rapid assessment of deposition changes resulting from fuel additives, different operating conditions, and coal type. This paper reports results from a drop-tube combustor specially developed to quantify the sticking coefficient as a function of operating conditions with fuel additives, for example. The present results identify temperature conditions that produce a low sticking coefficient and a low deposit strength. In addition, a modest computer simulation of the ash transport process confirms the experimental evidence, showing that large ash particles are relatively unaffected by surface cooling, while smaller particles may be cooled significantly in the thermal boundary layer above cooled hardware surfaces.

Experimental Procedure

Deposition experiments were performed in the combustion/deposition entrained reactor (CDER). A detailed description of the CDER and experimental procedure is given elsewhere (Anderson et al., 1988). The CDER is essentially an electrically heated drop-tube furnace with an exit nozzle designed to produce a high-velocity jet of combustion gases (Fig. 2). The CDER is capable of operating at pressures up to 12 atm, but the current results were obtained at 1 atm.

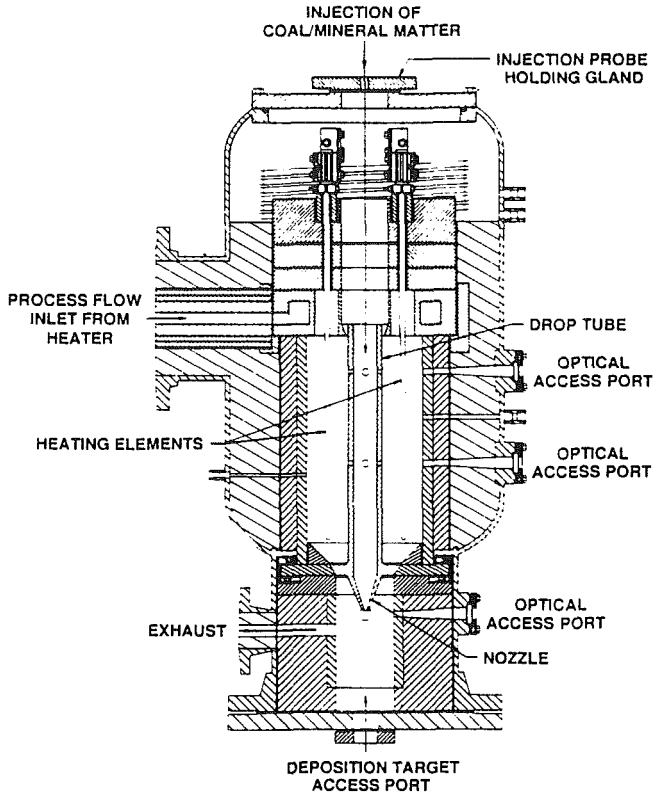

Fig. 2 Combustion/deposition entrained reactor (CDER)

Dry coal is injected into the top of the reactor and passes through the drop-tube region, where electric heaters allow careful control of the combustion temperature. Combustion temperatures reported here are measured with a type-K thermocouple, which contacts the drop tube exterior just above the optical access port. The process flow entering the reactor is heated to the temperature indicated by this thermocouple so that the drop tube interior is essentially isothermal, except for a short mixing region near the top. Coal/mineral matter is conveyed into the top of the drop tube with ambient temperature air amounting to less than 10 percent of the total drop tube flow. Temperature traverses conducted just 5 cm below this point showed a small 50 K drop in the centerline temperature, which was subsequently flattened by the mixing and heat input from the hot drop-tube walls. Residence time in the drop tube is more than 400 ms.

At the exit of the combustion zone, the products of combustion are accelerated through a 3.2-mm-dia nozzle, creating a jet with a mean velocity of 300 m/s. This is similar to the velocity expected in the first stage of an operating gas turbine. The high-velocity jet is directed perpendicular to a deposition target located 6 mm below the nozzle exit (Fig. 3). The target is a removable 12.7-mm platinum disk, 0.254 mm thick. Platinum was chosen as an inert target material to eliminate specific surface reactions peculiar to any particular blade material. The target and nozzle configuration was developed according to the procedures recommended by Marple and Willeke (1976)

Nomenclature

C = particle specific heat, J/kg-°K
C_D = particle drag coefficient
d_p = particle diameter, m
h = convection coefficient, W/m^2-°K
Re = particle Reynolds number, diameter
T_g = gas temperature, °K
T_p = particle temperature, °K
u = radial gas velocity
V = vertical gas velocity
x = radial coordinate
y = vertical coordinate
μ = dynamic gas viscosity, N•S/m^2
ρ = gas density
ρ_p = particle density, kg/m^3

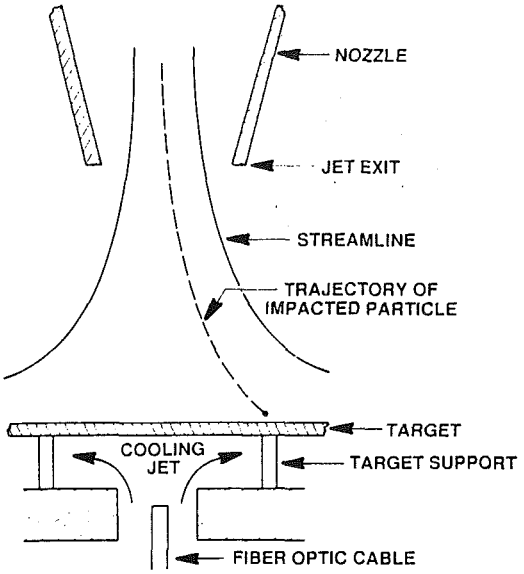

Fig. 3 CDER nozzle/target assembly

Table 1 Ash characteristics

	Arkwright Pittsburgh Bituminous	Blue Gem (Cleaned) Bituminous
% ASTM Ash	6.93	0.56
Ash Comp. (Wt%)		
SiO_2	48.09	16.86
Al_2O_3	25.07	22.75
Fe_2O_3	10.95	29.57
TiO_2	1.27	1.95
P_2O_5	0.18	0.48
CaO	5.78	7.03
MgO	1.25	2.46
K_2O	1.16	0.53
Na_2O	0.90	1.54
SO_2	5.34	8.07
Ash Fusion Temp. (K) (± 40)		
(Reducing Conditions)		
Initial Deformation	1,465	1,511
Softening	1,589	1,581
Hemispherical	1,629	1,644
Fluid	1,656	1,700

to ensure that all particles larger than 0.5 μm would be forced by inertia to impact the target rather than follow the gas streamlines. Figure 3 also shows that an opposing jet of cooling air can be supplied from an annular passage below the target. The center of the annulus is a sapphire rod in series with a fiber optic cable that monitors the target temperature through two-color pyrometry. The target temperatures reported here represent the temperature of the bottom of a clean target without the coal feed. Coal feed (and associated heat release) changed the measured temperature by less than 50 K, because the coal is deliberately supplied at a rate that is approximately 20 times more dilute than in an operating turbine. The dilute coal stream was chosen to allow long sampling times during deposition tests to improve the time resolution of ash deposit growth. A modest investigation of variations in the feed rate demonstrated little change in the measured sticking coefficient with higher coal feed rates.

Table 1 provides the ash composition for the two coals studied in the current investigation. The Arkwright bituminous is an uncleaned coal with almost 7 percent ash. The Blue Gem coal is a beneficiated bituminous coal with 0.56 percent ash. The major difference in composition between the two ashes is in the oxides of iron and silicon, with Arkwright having more silicon dioxide and less iron oxide than the Blue Gem coal. Despite these differences, the softening temperatures of the two coals are similar.

The Arkwright coal was used as a baseline fuel. The sticking fraction was measured by first quantifying the coal feed from quenched filter samples obtained at the nozzle exit. Quenching was accomplished by replacing the target assembly with a 47-mm, open-faced filter holder. Air injection at the periphery of the holder was used in conjunction with a vacuum pump to draw gasses through the filter. The cold air injection served to extinguish combustion of any unburned carbon. Samples collected in this manner showed that the resulting ash contained anywhere from 0.5 to 25 percent carbon, depending on the combustion temperature. As discussed elsewhere (Ahluwalia et al., 1989), the unburned carbon that survives low-temperature combustion can adhere to the deposit where it will have sufficient time to complete burning. The sticking fraction, S, is then computed from the ratio of ash (excluding unburned carbon), which is collected on the filter, versus the ash that adheres to the target during the same time interval:

$$S = \frac{\text{mass of ash adhering to target}}{\text{mass of ash (excluding unburned carbon) on filter sample}}.$$

Initial tests were conducted to establish the behavior of sticking coefficient versus time. Sticking data were obtained at times from 2 to 20 min for Arkwright coal, at reactor temperatures of 1373 and 1573 K. Results shown in Fig. 4 demonstrate that the sticking coefficient was approximately constant after 10 min, but was either larger or smaller after only 2 min, depending on the reactor temperature. Error bars included on this plot demonstrate that excellent data reproducibility was achieved in the CDER tests for times longer than 5 min. Thus, the study of sticking coefficient versus time suggested that 10-min test intervals would provide the most representative data for this investigation, and subsequent sticking data will refer to the 10-min test. While the sticking behavior could admittedly change for operation over many hours, it is not meaningful to consider longer tests until means are found to reduce the sticking coefficient below current levels.

As previously mentioned, the deposition tests were conducted with the coal feed deliberately supplied in a dilute form. Operating gas turbines could be expected to burn fuel at an overall (i.e., postdilution) equivalence ratio of 0.3. The current investigation was conducted at an equivalence ratio of 0.015. These dilute conditions were studied so that the reactor temperature could be easily characterized, controlled only by the electric heaters, and (almost) unaffected by the coal heat release. It is also noted that most proposed coal-fired turbine systems (Kothari and Rekos, 1988) include some form of particulate control (filters or cyclones), so that the product stream would have a very low particle concentration. While it was suspected that dilute conditions would merely slow the particle arrival rate (and thus not affect the fraction that stuck), it was noted that concomitant changes in the partial pressure of gaseous species might alter the sticking data by promoting condensation of gases responsible for liquid-phase adhesion. Figure 5 presents the measured sticking coefficient for Blue Gem coal and suggests that the fraction of adhering ash is approximately independent of the equivalence ratio, except at the highest feed rate for the 1373 K data, where the sticking coefficient is modestly reduced. However, the scatter in the data shows that the sticking fraction was somewhat erratic at the highest feed rates. Equivalence ratios higher than those shown in Fig. 5 were attempted but abandoned because of problems in feeding and mixing the fuel in the drop tube. The higher feed rates produced a jet of coal dust from the fuel injection probe, which resisted rapid mixing and, therefore, produced more

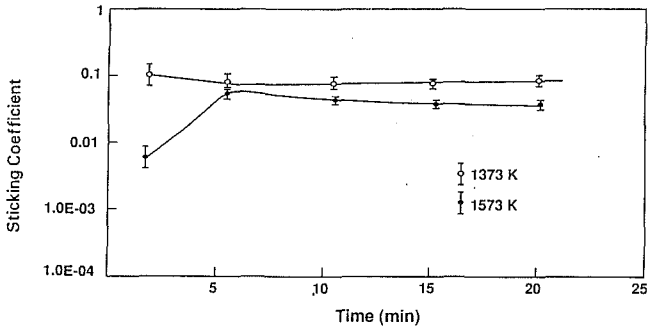

Fig. 4 Sticking coefficient versus time (Arkwright coal)

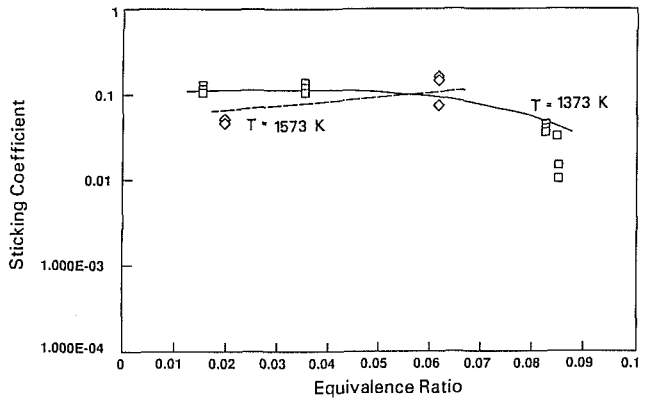

Fig. 5 Sticking versus equivalence ratio (Blue Gem coal)

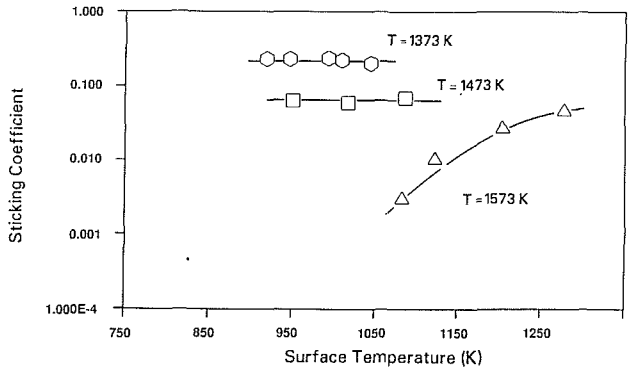

Fig. 6 Effect of surface temperature on sticking coefficient (Arkwright coal)

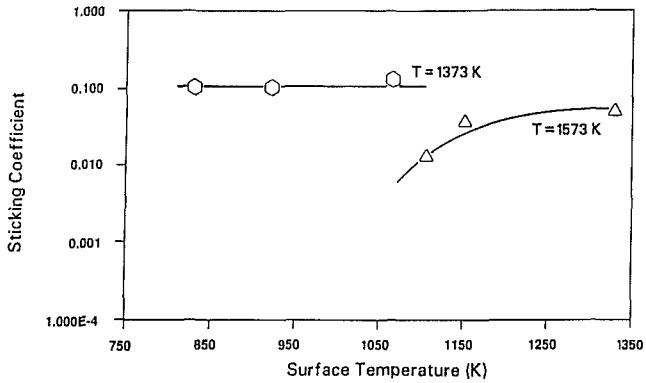

Fig. 7 Effect of surface temperature on sticking coefficient (Blue Gem coal)

unburned carbon in the depositing ash. The difficulties in feed rate and mixing were best avoided by operating the system in a dilute manner, and all subsequent discussion will be referenced to an equivalence ratio of 0.015.

Combined Effects of Surface Temperature and Combustion Temperature

Figures 6 and 7 present sticking coefficient data for the Arkwright and Blue Gem coals over a range of surface temperatures. The individual curves are referenced to the gas temperature in the drop tube (effectively the combustion temperature, since the dilute operation assures isothermal gas temperatures through the reaction region). Referring first to the data obtained at the low gas temperature of 1373 K, the sticking coefficient was unaffected by changes in the target surface temperature. Data for the Arkwright coal were also obtained at a gas temperature of 1473 K, and again the sticking coefficient was independent of the surface temperature but had a slightly smaller magnitude than at 1373 K gas temperature. Finally, at the highest gas temperature of 1573 K, both the Arkwright and Blue Gem coals showed a significant reduction in sticking coefficient as the surface temperature was cooled from 1250 K to 1050 K. This effect was more pronounced for the Arkwright coal than for the Blue Gem coal. However, the qualitative behavior of both coals was the same: at low combustion temperatures, the surface cooling had no effect on sticking coefficient; at higher combustion temperatures, surface cooling produced a significant reduction in the fraction of adhering ash. The reduction in sticking coefficient with surface temperature was expected from experience in boiler deposition (Raask, 1985), and also from recent deposition tests on gas turbine simulators (Ahluwalia et al., 1989). However, the data obtained at lower combustion temperatures (1373 K and 1473 K) were unexpected both because the sticking coefficient was independent of the surface temperature, and also because the magnitude of the sticking coefficient was smaller at higher combustion temperatures. It is possible that the higher combustion temperatures serve to vaporize molten species that would otherwise be present to promote adhesion. However, this would not explain why the low-temperature products of combustion were insensitive to surface cooling.

This distinctive behavior prompted further investigation. It was recognized that unlike the previous gas turbine simulator tests (Ahluwalia et al., 1989; Spiro et al., 1989), the depositing ash at each gas temperature experienced a unique combustion history and was, therefore, suspected to be physically and chemically disparate at the different gas temperatures. In fact, evidence for such a distinction was recognized early in the test program, where a noticeable difference in the appearance and character of the ash deposit was clearly evident at the various combustion temperatures. To investigate these differences, quenched ash samples were obtained on a standard filter with high (cold) air dilution and vacuum suction to quench and capture ash just after exiting the nozzle. Table 2 presents the fraction of unburned carbon for the Arkwright and Blue Gem coals at various combustion temperatures. The table shows that the low-temperature ash (1373 K) contained up to 20.8 percent unburned carbon, while the carbon content of the high-temperature ash was much less. Further differences in the nature of the deposit were evident when attempting to clean the platinum deposition targets for subsequent trials. The deposits obtained from low-temperature combustion (1373 K) were easily removed and exhibited a granular character that was readily pulverized. Conversely, high-temperature combustion (1573 K) produced strongly bonded deposits that were somewhat glassy.

These differences in the character of the deposit raise some interesting issues. The data in Figs. 6 and 7 show that higher

Table 2 Carbon content of ash

	Combustion Temperature (K) 1373	1573
Arkwright	20.8%	0.9%
Blue Gem	16.7%	5.0%

temperature combustion and surface cooling can produce a lower sticking coefficient. However, as previously explained, the smaller fraction of ash that did stick was tightly bonded to the hardware. In practice, reductions in the sticking coefficient must be weighed against the ability to remove the deposit during turbine maintenance. Deposition control strategies would thus seem to benefit from consideration of both the sticking coefficient and the deposit adhesion strength. A preliminary paper from this laboratory (Richards et al., 1988) has reported initial efforts to characterize deposit strength concurrent with the sticking measurements now in progress. Again, although the current data demonstrate a reduction in sticking coefficient by higher combustion temperatures, the adhering ash is bonded tightly to the metal surface, perhaps offsetting the advantage of a reduced sticking coefficient.

To assess further the difference in ash properties at the different combustion temperatures, scanning electron micrographs of the quenched ash samples were obtained. The micrographs revealed some physical differences in the ash produced at different temperatures, but the most notable difference was recognized when the micrographs were used to produce particle-size distributions by digital image analysis. A mass distribution was produced from the image analysis by weighing the size distribution with the cube of the diameter. The mass size distribution thus obtained (for Arkwright coal) is plotted in Fig. 8 and clearly demonstrates a shift in mass size distribution at the two combustion temperatures. The high-temperature combustion produced ash with particle sizes all less than 20 μm in diameter, and with a peak in the mass distribution just above 5 μm. Conversely, much of the low-temperature ash was concentrated in the large particles between 10 and 40 μm. A very small fraction of the ash was contained in particles smaller than 5 μm.

In terms of the observed sticking data, these differences in mass size distribution suggest the following hypothesis. The sticking coefficient data obtained at low combustion temperatures were insensitive to surface cooling, because the relatively large particles could not be cooled before impacting on the deposit surface. On the other hand, the small particles associated with high-temperature combustion could be quenched as they passed through the thermal boundary layer adjacent to the cooled deposition surface. If, for example, the mechanism of particle adhesion is attributed to some molten phases, it is possible that cooling of the small particles would solidify molten phases and reduce the sticking coefficient at high combustion temperatures. Molten phases would not solidify at low combustion temperatures, because the majority of large particles could not adjust to the rapid temperature change as they pass through the boundary layer.

To explore these possibilities, an approximate model of both the flow and particle trajectories in the nozzle/target region was constructed. While a more detailed finite difference solution to the flow and thermal fields could be obtained as in Marple and Liu (1974), such refinement was not needed in the present calculations, where the goal was merely to confirm physical insight into the deposition process for small and large particles as previously described. Furthermore, uncertainties in particle shape and density make refined flow calculations of uncertain value in predicting particle trajectories. As such, the flow and thermal fields were modeled as an axisymmetric,

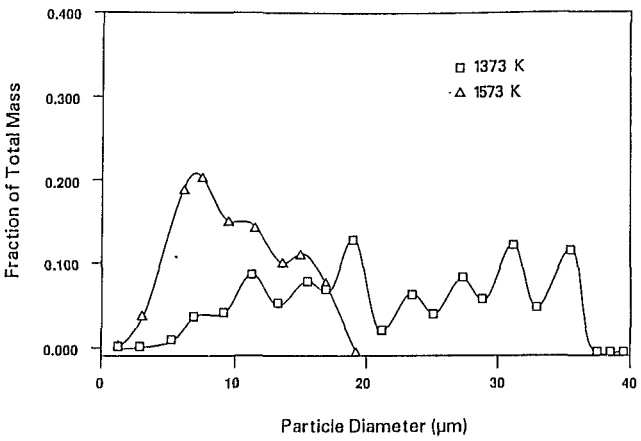

Fig. 8 Ash particle mass distribution (Arkwright coal)

potential stagnation flow coupled to a boundary layer stagnation flow. This approach allowed the flow field to be written as a direct function of location through the standard Blasius solution within the boundary layer (Schlichting, 1979), having boundary conditions imposed to meet the external potential flow solution. Having thus described the flow and thermal fields, the local gas velocity and temperature were used as inputs to the equations of particle motion and thermal energy:

$$\ddot{x}=\frac{3}{4}C_D\,\mathrm{Re}\,\frac{\mu}{\rho_p d_p^2}(u-\dot{x}), \tag{1}$$

$$\ddot{y}=\frac{3}{4}C_D\,\mathrm{Re}\,\frac{\mu}{\rho_p d_p^2}(v-\dot{y}), \text{ and} \tag{2}$$

$$T_p=\frac{6h}{\rho_p d_p C}(T_g-T_p). \tag{3}$$

The convection coefficient, h, was obtained from standard correlations for spheres (Bird et al., 1960). The equations of motion utilize a drag coefficient that was calculated from empirical expressions for C_D as in Morsi and Alexander (1972). Equations (1)–(3) were numerically integrated over time steps of 1 μs in the potential flow region, and 0.1 μs inside the boundary layer. Calculations were started with the particle gas velocity equal to characteristic velocities in the CDER experiments at the nozzle exit (300 m/s) and at the highest gas temperature studied (1573 K). The particle trajectories began at the same nozzle target separation as exists in the CDER experiments. Trajectories were started at 0.01 nozzle radii from the center line. The potential/boundary layer flow model used here is not an exact representation of the flow field in the CDER, but can be expected reasonably to mimic the behavior near the flow centerline where edge effects are minimal. Results of these calculations are shown in Fig. 9, where particle trajectories within the boundary layer are plotted for 1.25 and 2.50 μm (diameter) particles. The coordinate axes in this figure are made dimensionless with the nozzle/target separation. As the figure shows, particle trajectory is greatly affected by the particle diameter. The twofold increase in diameter represents an eightfold increase in particle mass. The trajectories reflect the increased inertia of the larger particle, which impacts the target essentially perpendicularly, while the smaller particle is diverted noticeably by the radial gas velocity. Similar distinctions are evident in the particle temperature history shown in Fig. 10. In this figure, the horizontal axis is the particle temperature as the particle drops through the vertical coordinate (dimensionless height). The deposition surface was maintained at 1050 K in these calculations, just as in the CDER experiments (i.e., the high combustion temperature, 1573 K) and cooled surface (1050 K). As seen in the figure, target cooling can effectively cool the smaller particle, but not the larger particle.

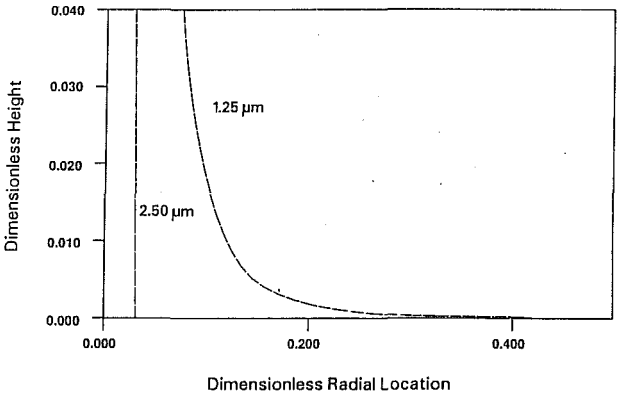

Fig. 9 Ash particle trajectory for 1.25 and 2.5-μm-dia particles

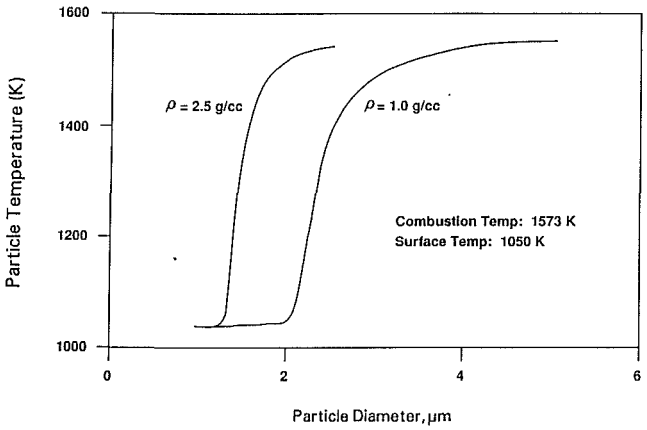

Fig. 11 Ash particle temperature at impact

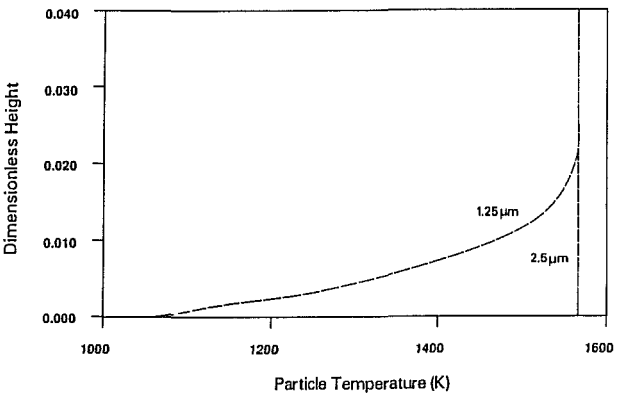

Fig. 10 Ash particle temperature history for 1.25 and 2.5-μm-dia particles

The 2.5 μm particle arrives at the surface unaffected by the surface cooling, while the 1.25 μm particle is cooled to the surface temperature before impacting.

The above calculations are dependent on a number of parameters that are difficult to characterize. For example, the particle drag coefficient is undoubtedly affected by the irregular particle shape, while the particle density and specific heat may be complicated by the mineral ash composition and structure. These differences will contribute to a quantitative change in the results of the calculation, but the qualitative behavior is unchanged. For example, Fig. 11 shows the temperature of impacting ash particles of different sizes when they impact the deposition surface. Conditions are as shown on the figure, with results plotted for two different particle densities. Referring first to the smaller density of 1 g/cc, the results show that all particles smaller than 2 μm will arrive at the surface cooled to the surface temperature. Particles larger than 4 μm will be thermally unaffected by the transit through the cool boundary layer. Similar behavior is observed at the larger density of 2.5 g/cc, but the relative sizes are reduced.

With regard to the experimental data, it is interesting to note that the above calculations demonstrate that small particles can be quenched in the thermal boundary layer adjacent to hardware surfaces. However, because of the high velocities associated with turbine applications, it is likely that the larger particles cannot be cooled in the relatively brief passage through the thermal boundary layers. No specific critical size for particle cooling is stated in the present investigation, because the critical size will obviously change in different flow geometries and flow velocities. While it is difficult to characterize a critical size for cooling, even with a generous choice for all unknown parameters in the current tests, large particles (i.e., larger than 10 μm) will arrive at the surface essentially uncooled. Referring again to the experimental mass distribution for low-temperature combustion (Fig. 8), it is evident that most of the impacting ash will arrive at the deposition surface unaffected by surface cooling. Assuming that ash adhesion is promoted by soft or molten material constituting the ash, the calculations may explain why the sticking coefficient was independent of surface temperature at the low combustion temperature (Figs. 6 and 7). Because the majority of the mass occurs in large particles, the molten components responsible for adhesion cannot be frozen in the transition through the boundary layer. Conversely, the high-temperature combustion products are characterized by many particles smaller than 5 μm (Fig. 8), and molten phases associated with these small particles could be effectively frozen during transition through the thermal boundary layer. This behavior may explain the reduction in deposition observed experimentally for the high-temperature combustion products where surface cooling was observed to reduce the sticking coefficient.

Conclusions

The data and calculations suggest that a proper combination of combustion history and hardware surface temperature can contribute to effective deposition mitigation in coal-burning turbines. If the combustion history is such that most of the remaining ash is in large particles, surface cooling will be unable to quench arriving ash particles, and the sticking coefficient could be unaffected by surface cooling. However, if the combustion process is tailored to produce fine ash particles, the surface cooling can be very effective at reducing deposition. A critical size for effective cooling is not presented in the present analysis, because this size is dependent on a number of parameters that are difficult to characterize and will vary with flow geometry and coal ash type. It is also observed that the combustion temperature plays a role in determining the strength of the ash deposit. Although the low-temperature combustion produces a greater sticking coefficient, the ash deposits are weakly bonded and can be easily removed. This suggests that a trade-off between sticking coefficient and deposit strength may be needed to ensure that a minimal quantity of ash adheres to hardware, and also that the ash, which does stick, can be removed by on- or off-line cleaning.

References

Ahluwalia, R. K., Im, K. H., and Wenglarz, R. A., 1989, "Flyash Adhesion in Simulated Coal-Fired Gas Turbine Environment," ASME JOURNAL OF ENGINEERING FOR GAS TURBINES AND POWER, Vol. 111, pp. 672–678.

Anderson, R. J., Meyer, C. T., and Dennis, R. A., 1988, "A Combustion/Deposition Entrained Reactor for High Temperature/Pressure Studies of Coal

and Coal Minerals," presented at the 1988 Annual AIChE Meeting, Washington, DC, Nov. 27–Dec. 2.

Benson, S. A., Tangsathitkulchai, M., and Austin, L. G., 1985, "Studies of Ash Deposit Formation Using a Laboratory Furnace," *Proceedings of the Second Annual Pittsburgh Coal Conference*, p. 689.

Bird, R. B., Stewart, W. E., and Lightfoot, E. N., 1960, *Transport Phenomena*, Wiley, New York.

France, J. E., Grimm, U., Anderson, R. J., and Kovach, J. J., 1984, *Deposition and Corrosion in Gas Turbines Utilizing Coal or Coal-Derived Fuel*, DOE/METC/84-17 (DE84009290).

Kothari, V., and Rekos, N., 1988, *Proceedings of the Annual Coal-Fuel Heat Engines and Gas Stream Cleanup System Contractors Review Meeting*, DOE/METC-88/6094, NTIS/DE88001088, CONF-880656.

Marple, V. A., and Liu, Y. H., 1974, "Characteristics of Laminar Jet Impactors," *Environmental Science and Technology*, Vol. 8, pp. 648–654.

Marple, V. A., and Willeke, K., 1976, "Impactor Design," *Atmospheric Environment*, Vol. 10, pp. 891–896.

Morsi, S. A., and Alexander, A. J., 1972, "Theoretical Low Speed Particles Collision With Symmetrical and Cambered Aerofoils," ASME Paper No. 72-WA/FE-35.

Raask, E., 1985, *Mineral Impurities in Coal Combustion*, Hemisphere Publishing, Washington, DC.

Richards, G., Logan, R., Meyer, C., and Anderson, R. J., 1988, "Deposition Effects in Pressurized Combustion of Coal-Derived Fuels," *Proceedings of the AR&TD Direct Utilization and Instrumentation and Diagnostics Contractors Review Meeting*, sponsored by U.S. Department of Energy, Pittsburgh Energy Technology Center, Sept. 6–9, Pittsburgh, PA.

Rosner, D. E., and Nagarajan, R., 1987, "Toward a Mechanistic Theory of Net Deposit Growth From Ash-Laden Flowing Combustion Gasses: Self-Regulated Sticking of Impacting Particles and Deposit Erosion in the Presence of Vapor Glue," *24th National Heat Transfer Conference*, AIChE Symposium Series, Vol. 3, No. 257, pp 289–296.

Ross, J. S., Anderson, R. J., and Nagarajan, R., 1988, "Effect of Sodium Deposition in a Simulated Combustion Gas Turbine Environment," *J. Energy and Fuels*, Vol. 2, pp. 282–289.

Schlichting, H., 1979, *Boundary Layer Theory*, McGraw-Hill, New York.

Spiro, C. L., Chen, C. C., Kimura, S. G., Lavigne, R. G., and Schields, P. W., 1989, "Deposit Remediation in Coal-Fired Gas Turbines Through the Use of Additives," ACS Division of Fuel Chemistry, preprints of papers presented at the ACS National Meeting in Dallas, TX, Vol. 34, No. 2.